Supermultiplet structure of the doubly excited positronium negative ion

I. A. Ivanov* and Y. K. Ho
Institute of Atomic and Molecular Sciences, Academia Sinica, P.O. Box 23-166, Taipei, Taiwan, Republic of China
(Received 13 August 1999; published 10 February 2000)

Doubly excited intrashell resonance states of positronium negative ion, Ps^- associated with the $N=4$ and $N=5$ thresholds of Ps atom are calculated using the method of complex-coordinate rotation. Products of Slater-type orbitals are used to represent the two-electron wave functions. All possible intrashell states with angular momenta up to $L=6$ and $L=8$ for $N=4$ and $N=5$ thresholds, respectively, have been identified. Supermultiplet structures showing the rotational and vibrational character of the doubly excited resonance states of Ps^- are constructed.

PACS number(s): 36.10.Dr, 32.80.Dz, 31.25.Jf

I. INTRODUCTION

Positronium negative ion Ps^- is a member of the family of the three-body atomic systems interacting through the Coulomb forces. There has been a considerable amount of works devoted to the studies of the resonances in e-Ps scattering associated with the $N=2$ positronium threshold. Theoretical methods such as the complex-coordinate rotation method [1,2], the Kohn variational method [3], adiabatic treatment in the hyperspherical coordinates [4], adiabatic molecular approximation [5], and the hyperspherical close coupling method [6,7] have been used in these works. For H^- it is well known, that the $^3P^e$ state associated with the $N=2$ threshold lies below the threshold and is in fact a metastable state. Therefore, it is called sometimes the second ''bound'' state in H^-. The absence of such a ''bound state'' in Ps^- was established by Mills [8] as well as by Bhatia and Drachman [9] using a variational method, and by Botero [10] with the use of the adiabatic potential curves. Both resonance position and width for the $^3P^e$ state [which can be identified as a shape resonance lying above the Ps ($N=2$) threshold] were determined using the method of complex-coordinate rotation [11]. For the resonances associated with the $N=3$ Ps threshold, there are works using the complex-coordinate rotation method [2,12], adiabatic molecular approximation [5], and the hyperspherical close coupling method [7]. For resonances associated with higher Ps thresholds, the method of the complex-coordinate rotation is the preferred tool as there is no need to include channel-by-channel representations for the wave functions. The calculation of the resonance position and the total width for a multichannel resonance is as straightforward as that for a one-channel resonance. Accurate calculations of S, P, and D-wave resonances up to the Ps ($N=7$) threshold have been performed [11,13–15] with Hylleraas basis functions.

In addition to the theoretical interest, this exotic system has also attracted experimental interest, as it was produced by Mills in the laboratory [16]. The annihilation rate for Ps^- was also subsequently measured [17]. These experimental activities contribute partly to the motivation for theorists to investigate this nontrivial atomic system.

We have recently carried out a calculation of some high angular-momentum ($L\geqslant 3$) doubly excited states of Ps^- using the method of complex coordinate rotation [18]. We reported the results for all the doubly excited intrashell states associated with the Ps ($N=3$) threshold, as well as for several states associated with the lowest rotor series that are converging to the Ps ($N=4$) and Ps ($N=5$) thresholds.

In the present work, we report the results for all the doubly excited intrashell states associated with the Ps ($N=4$) and Ps ($N=5$) thresholds. Our results are used to construct the supermultiplet structures of doubly excited states of Ps^-.

Finally we mention that studies of the ground state of Ps^- were carried out in Ref. [19]. Earlier investigations were reviewed in Refs. [12,20–23]. In the present work a complex-coordinate rotation [24] calculation using products of Slater-type orbitals (STO's) to represent the two-electron wave functions is carried out. It is believed that for doubly excited states with high angular momentum $L\geqslant 3$, the two electrons are pushed apart by the angular momentum barrier. The omission of the Hylleraas r_{12} (interparticle) factor in calculations of resonance parameters of such states should not be as crucial as for the lower angular momentum states. The use of separable products STO can therefore be expected to provide accurate results. Our results for the resonances with $L\leqslant 2$ can be compared with the earlier Hylleraas results, by means of such comparison the accuracy can be checked. In the following, we will present results for doubly excited intrashell (both electrons occupy the same shell) and intershell states associated with the Ps $N=4$ and $N=5$ thresholds. In addition, our present results are used to construct supermultiplet structures of doubly excited Ps^-.

II. WAVE FUNCTIONS AND CALCULATIONAL PROCEDURE

If one introduces the relative coordinates $\vec{r}_1,\vec{r}_2$ of electrons with respect to the positron, and the distance $\vec{r}_{12}$ between two electrons, the Hamiltonian of Ps^- can be written as (rydberg units are used)

$$H=T+V \tag{1}$$

with $T=-2\nabla_1^2-2\nabla_2^2-2\vec{\nabla}_1\cdot\vec{\nabla}_2$ and $V=-2/r_1-2/r_2+2/r_{12}$.

*On leave from the Institute of Spectroscopy.

TABLE I. Comparison of the present results and results of the Hyleraas basis calculation for the resonances of $^1S^e$ symmetry associated with $N=4$ and $N=5$ thresholds.

	State	Present results		Results from Ref. [12]	
		E_r(Ry)	$\Gamma/2$(Ry)	E_r(Ry)	$\Gamma/2$(Ry)
$N=4$	$^1S^e$ (1)	-0.04042797 (10^{-8})	1.3012×10^{-4}	-0.04042783	1.3009×10^{-4}
	$^1S^e$ (2)	-0.0350207 (1×10^{-7})	1.315×10^{-4}	-0.0350208	1.315×10^{-4}
	$^1S^e$ (3)	-0.034621764 (5×10^{-9})	1.57917×10^{-4}	-0.03462187	1.5782×10^{-4}
$N=5$	$^1S^e$ (1)	-0.02606180 (2×10^{-8})	1.0529×10^{-4}	-0.02606188	1.0512×10^{-4}
	$^1S^e$ (2)	-0.02344559 (5×10^{-8})	4.347×10^{-5}	-0.02344563	4.344×10^{-5}
	$^1S^e$ (3)	-0.0230390 (10^{-7})	1.164×10^{-4}	-0.0230391	1.163×10^{-4}
	shape	-0.0198822 (5×10^{-7})	2.23×10^{-5}	-0.019875	1.9×10^{-5}

TABLE II. Doubly excited intrashell states of Ps- associated with the Ps ($N=4$) threshold (threshold energy$=-0.03125$ Ry). The estimated uncertainty in the resonance energy is given in the parentheses.

State	$KTNn$	E_r(Ry)	$\Gamma/2$(Ry)	Resonance
$^1S^e$	3044	-0.04042797 (10^{-8})	1.3012×10^{-4}	Feshbach
$^3P^o$	3044	-0.04016744 (10^{-8})	1.1987×10^{-4}	Feshbach
$^1D^e$	3044	-0.0396432 (3×10^{-7})	9.77×10^{-5}	Feshbach
$^3F^o$	3044	-0.0388329 (3×10^{-7})	6.49×10^{-5}	Feshbach
$^1G^e$	3044	-0.0377407 (3×10^{-7})	3.46×10^{-5}	Feshbach
$^3H^o$	3044	-0.0363291 (5×10^{-7})	2.05×10^{-5}	Feshbach
$^1I^e$	3044	-0.0347208 (5×10^{-7})	7.51×10^{-5}	Feshbach
$^1P^o$	2144	-0.03778077 (2×10^{-8})	3.079×10^{-5}	Feshbach
$^3D^e$	2144	-0.03707594 (5×10^{-8})	5.874×10^{-5}	Feshbach
$^1F^o$	2144	-0.0360023 (10^{-7})	1.167×10^{-4}	Feshbach
$^3G^e$	2144	-0.0346804 (10^{-7})	1.538×10^{-4}	Feshbach
$^1H^o$	2144	-0.0331262 (5×10^{-7})	7.76×10^{-5}	Feshbach
$^3P^e$	2144	-0.03778921 (10^{-8})	1.511×10^{-5}	Feshbach
$^1D^o$	2144	-0.03709893 (10^{-8})	2.382×10^{-5}	Feshbach
$^3F^e$	2144	-0.0360326 (2×10^{-7})	6.65×10^{-5}	Feshbach
$^1G^o$	2144	-0.0347117 (10^{-7})	1.087×10^{-4}	Feshbach
$^3H^e$	2144	-0.0331085 (2×10^{-7})	4.55×10^{-5}	Feshbach
$^1D^e$	1244	-0.0344947 (4×10^{-7})	1.848×10^{-4}	Feshbach
$^3F^o$	1244	-0.0332346 (5×10^{-7})	6.88×10^{-5}	Feshbach
$^1G^e$	1244	-0.031905 (10^{-6})	9.2×10^{-5}	Feshbach
$^3D^o$	1244	-0.03450125 (10^{-8})	1.8066×10^{-4}	Feshbach
$^1F^e$	1244	-0.0332336 (10^{-7})	6.97×10^{-5}	Feshbach
$^3G^o$	1244	-0.031867 (10^{-6})	3.2×10^{-5}	Feshbach
$^1F^o$	0344	-0.030935 (3×10^{-6})	1.73×10^{-4}	shape
$^3F^e$	0344	-0.030937 (3×10^{-6})	1.58×10^{-4}	shape
$^1S^e$	1044	-0.034621764 $(5\times10-9)$	1.57917×10^{-4}	Feshbach
$^3P^o$	1044	-0.03425951 (5×10^{-8})	1.6559×10^{-4}	Feshbach
$^1D^e$	1044	-0.0334948 (5×10^{-7})	1.171×10^{-4}	Feshbach
$^3F^o$	1044	-0.032187 (5×10^{-6})	7.8×10^{-5}	Feshbach
$^1G^e$	1044	-0.03097 (10^{-5})	1.3×10^{-4}	Feshbach
$^1P^o$	0144	-0.030955 (3×10^{-6})	6.1×10^{-5}	shape
$^3D^e$	0144	-0.030199 (5×10^{-6})	4.58×10^{-4}	shape
$^1F^o$	0144	-0.02902 (10^{-5})	1.27×10^{-3}	shape
$^3P^e$	0144	-0.030967 (10^{-6})	4.2×10^{-5}	shape
$^1D^o$	0144	-0.0302019 (5×10^{-7})	4.017×10^{-4}	shape
$^3F^e$	0144	-0.029000 (10^{-5})	1.14×10^{-3}	shape

TABLE III. Doubly excited intrashell states of Ps- associated with the Ps ($N=5$) threshold (threshold energy$=-0.02$ Ry). The estimated uncertainty in the resonance energy is given in the parentheses.

State	$KTNn$	E_r(Ry)	$\Gamma/2$(Ry)	Resonance
$^1S^e$	4055	$-0.02606180\ (2\times10^{-8})$	1.0529×10^{-4}	Feshbach
$^3P^o$	4055	$-0.0259628\ (3\times10^{-7})$	1.034×10^{-4}	Feshbach
$^1D^e$	4055	$-0.0257659\ (2\times10^{-7})$	1.002×10^{-4}	Feshbach
$^3F^o$	4055	$-0.0254700\ (8\times10^{-7})$	9.21×10^{-5}	Feshbach
$^1G^e$	4055	$-0.025068\ (2\times10^{-6})$	7.9×10^{-5}	Feshbach
$^3H^o$	4055	$-0.024556\ (10^{-6})$	5.0×10^{-5}	Feshbach
$^1I^e$	4055	$-0.023916\ (2\times10^{-6})$	2.7×10^{-5}	Feshbach
$^3K^o$	4055	$-0.023158\ (10^{-6})$	1.3×10^{-5}	Feshbach
$^1L^e$	4055	$-0.022295\ (3\times10^{-6})$	2.8×10^{-5}	Feshbach
$^1P^o$	3155	$-0.0249259\ (10^{-7})$	3.05×10^{-5}	Feshbach
$^3D^e$	3155	$-0.0246575\ (5\times10^{-8})$	3.723×10^{-5}	Feshbach
$^1F^o$	3155	$-0.02425339\ (10^{-8})$	4.841×10^{-5}	Feshbach
$^3G^e$	3155	$-0.0237356\ (2\times10^{-7})$	6.27×10^{-5}	Feshbach
$^1H^o$	3155	$-0.0230810\ (10^{-7})$	5.83×10^{-5}	Feshbach
$^3I^e$	3155	$-0.0223070\ (7\times10^{-7})$	9.06×10^{-5}	Feshbach
$^1K^o$	3155	$-0.021509\ (2\times10^{-6})$	9.5×10^{-5}	Feshbach
$^3P^e$	3155	$-0.024931662\ (2\times10^{-9})$	2.5467×10^{-5}	Feshbach
$^1D^o$	3155	$-0.02467219\ (10^{-8})$	2.305×10^{-5}	Feshbach
$^3F^e$	3155	$-0.02427477\ (5\times10^{-8})$	2.087×10^{-5}	Feshbach
$^1G^o$	3155	$-0.0237579\ (10^{-7})$	2.828×10^{-5}	Feshbach
$^3H^e$	3155	$-0.0231079\ (10^{-7})$	2.35×10^{-5}	Feshbach
$^1I^o$	3155	$-0.0223285\ (10^{-7})$	5.70×10^{-5}	Feshbach
$^3K^e$	3155	$-0.0215083\ (5\times10^{-7})$	7.06×10^{-5}	Feshbach
$^1D^e$	2255	$-0.0234078\ (10^{-7})$	5.34×10^{-5}	Feshbach
$^3F^o$	2255	$-0.02293568\ (5\times10^{-8})$	6.508×10^{-5}	Feshbach
$^1G^e$	2255	$-0.022309\ (3\times10^{-6})$	1.13×10^{-4}	Feshbach
$^3H^o$	2255	$-0.2158395\ (5\times10^{-7})$	9.61×10^{-5}	Feshbach
$^1I^e$	2255	$-0.02079\ (2\times10^{-5})$	9.8×10^{-5}	Feshbach
$^3D^o$	2255	$-0.02340822\ (10^{-8})$	5.381×10^{-5}	Feshbach
$^1F^e$	2255	$-0.0229361\ (10^{-7})$	6.85×10^{-5}	Feshbach
$^3G^o$	2255	$-0.0223185\ (5\times10^{-7})$	1.138×10^{-4}	Feshbach
$^1H^e$	2255	$-0.0215791\ (10^{-7})$	9.63×10^{-5}	Feshbach
$^3I^o$	2255	$-0.02077\ (10^{-5})$	6.2×10^{-5}	Feshbach
$^1F^o$	1355	$-0.0217068\ (10^{-7})$	1.387×10^{-4}	Feshbach
$^3G^e$	1355	$-0.020955\ (10^{-6})$	5.7×10^{-5}	Feshbach
$^1H^o$	1355	$-0.02022\ (5\times10^{-5})$	1.6×10^{-4}	Feshbach
$^3F^e$	1355	$-0.0217069\ (10^{-7})$	1.392×10^{-4}	Feshbach
$^1G^o$	1355	$-0.0209530\ (5\times10^{-7})$	5.39×10^{-5}	Feshbach
$^3H^e$	1355	$-0.02028\ (3\times10^{-5})$	1.2×10^{-4}	Feshbach
$^1G^e$	0455	$-0.019869\ (2\times10^{-6})$	1.19×10^{-4}	shape
$^3G^o$	0455	$-0.019852\ (10^{-6})$	1.09×10^{-4}	shape
$^1S^e$	2055	$-0.02344559\ (5\times10^{-8})$	4.347×10^{-5}	Feshbach
$^3P^o$	2055	$-0.02330021\ (3\times10^{-8})$	5.149×10^{-5}	Feshbach
$^1D^e$	2055	$-0.0229991\ (10^{-7})$	6.01×10^{-5}	Feshbach
$^3F^o$	2055	$-0.022521\ (10^{-6})$	6.1×10^{-5}	Feshbach
$^1G^e$	2055	$-0.021960\ (5\times10^{-6})$	1.10×10^{-4}	Feshbach
$^3H^o$	2055	$-0.021308\ (5\times10^{-6})$	7.9×10^{-5}	Feshbach
$^1I^e$	2055	$-0.020616\ (5\times10^{-6})$	3.9×10^{-5}	Feshbach
$^1P^o$	1155	$-0.02166018\ (3\times10^{-8})$	1.3609×10^{-4}	Feshbach
$^3D^e$	1155	$-0.02135654\ (2\times10^{-8})$	1.1783×10^{-4}	Feshbach
$^1F^o$	1155	$-0.020809\ (5\times10^{-6})$	6.8×10^{-5}	Feshbach
$^3G^e$	1155	$-0.020137\ (3\times10^{-6})$	6.0×10^{-5}	Feshbach

TABLE III. (*Continued*).

State	$KTNn$	E_r(Ry)	$\Gamma/2$(Ry)	Resonance
$^1H^o$	1155	-0.01947 (10^{-5})	2.5×10^{-4}	shape
$^3P^e$	1155	-0.021659978 (5×10^{-9})	1.32025×10^{-4}	Feshbach
$^1D^o$	1155	-0.0213581 (10^{-7})	1.149×10^{-4}	Feshbach
$^3F^e$	1155	-0.020833 (5×10^{-6})	5.8×10^{-5}	Feshbach
$^1G^o$	1155	-0.020174 (10^{-6})	2.5×10^{-5}	Feshbach
$^3H^e$	1155	-0.01949 (10^{-5})	1.6×10^{-4}	shape
$^1D^e$	0255	-0.019785 (3×10^{-6})	5.4×10^{-5}	shape
$^3F^o$	0255	-0.019215 (10^{-6})	2.06×10^{-4}	shape
$^1G^e$	0255	-0.01851 (10^{-5})	6.9×10^{-4}	shape
$^3D^o$	0255	-0.019779 (10^{-6})	4.4×10^{-5}	shape
$^1F^e$	0255	-0.019238 (10^{-6})	2.81×10^{-4}	shape
$^3G^o$	0255	-0.018531 (3×10^{-6})	7.17×10^{-4}	shape
$^1S^e$	0055	-0.0198822 (5×10^{-7})	2.23×10^{-5}	shape
$^3P^o$	0055	-0.019710 (2×10^{-6})	5.3×10^{-5}	shape
$^1D^e$	0055	-0.019376 (5×10^{-6})	1.74×10^{-4}	shape
$^3F^o$	0055	-0.018868 (10^{-6})	4.45×10^{-4}	shape
$^1G^e$	0055	-0.01819 (10^{-5})	8.4×10^{-4}	shape

The description of the complex coordinate method and its application to the Ps^- system can be found elsewhere [24], here we shall outline briefly some details of the computational procedure used. The basis wave functions used in the present work are properly symmetrized products of the Slater-type orbitals

$$\Psi(\vec{r}_1,\vec{r}_2)=\phi_{n_1l_1}(r_1)\phi_{n_2l_2}(r_2)Y^{L,M}_{l_1,l_2}(1,2)S(\sigma_1,\sigma_2) - \phi_{n_1l_1}(r_2)\phi_{n_2l_2}(r_1)Y^{L,M}_{l_1,l_2}(2,1)S(\sigma_2,\sigma_1), \tag{2}$$

where

$$\phi_{nl}(r)=r^n\exp(-\xi_l r) \tag{3}$$

and $Y^{L,M}_{l_1,l_2}(1,2)$ and $S(\sigma_2,\sigma_1)$ are the eigenfunctions of total angular and spin momenta, respectively. They are constructed in a usual way, e.g., for $Y^{L,M}_{l_1,l_2}$ one has

$$Y^{L,M}_{l_1,l_2}(1,2)=\sum_{m_{l_1}m_{l_2}} C(l_1,l_2,L,m_{l_1},m_{l_2},M)Y_{l_1m_{l_1}}(1) \times Y_{l_2m_{l_2}}(2), \tag{4}$$

where $C(l_1,l_2,L,m_{l_1},m_{l_2},M)$ are the Clebsch-Gordan coefficients. The parameters n,l of the Slater orbitals are varied in the limits $0\leq l\leq N_{\max}$, $l\leq n\leq N_{\max}$ where the parameter $N_{\max}$ has the same value for both Slater orbitals in the formula (2). This parameter thus governs the size of the basis used in the calculation. Due to numerical problems the basis size cannot be chosen too large since for too large a basis the overlap matrix [i.e., the matrix of the scalar products of the

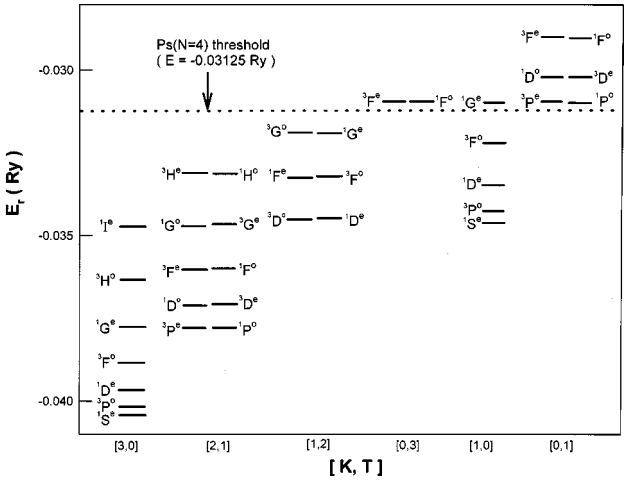

FIG. 1. Rotational character of the spectra of the doubly excited intrashell states of Ps^- associated with the Ps($N=4$) threshold.

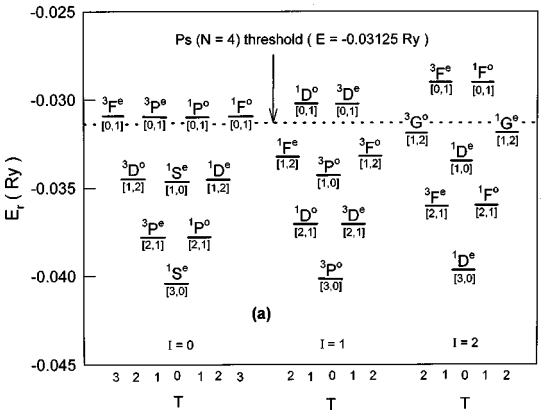

FIG. 2. Vibrational character of the spectra of the doubly excited intrashell states of Ps^- associated with the Ps($N=4$) threshold, I values ranging from $I=0$ to $I=2$.

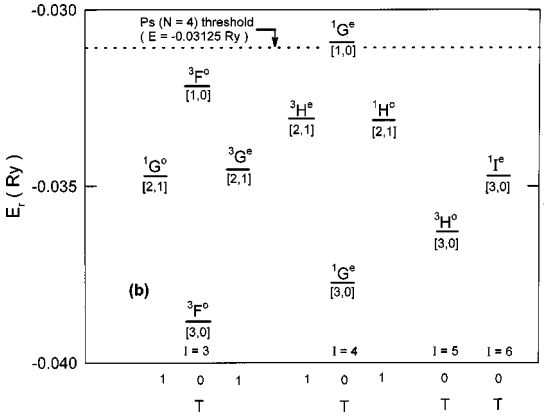

FIG. 3. Vibrational character of the spectra of the doubly excited intrashell states of Ps^- associated with the Ps($N=4$) threshold, I values ranging from $I=3$ to $I=6$.

functions given by Eq. (2)] becomes ill conditioned. The typical basis size used in the present calculation is 1200–1400 which corresponds to the values of the parameter $N_{\max}$: $14 \leqslant N_{\max} \leqslant 19$. Thus, for example in calculation of the $^1S^e$ resonance presented below, we use 19 individual *s* orbitals, 18 individual *p* orbitals, 17 *d* orbitals, 16 *f* orbitals, and so on, finishing with 1 orbital with $l=18$. Coupling and symmetrizing the products of these orbitals to construct two-electron basis functions of $^1S^e$ symmetry one obtains 1330 different basis functions.

The parameters ξ_l in Eq. (2) can be chosen independently for different l and can be used in the calculation as additional nonlinear variational parameters. In the present calculation of the lowest resonances of each symmetry, the ξ_l's are chosen to correspond to the ''positronium'' values. For example, when calculating the resonances associated with the $N=4$ positronium threshold the parameters ξ_l are chosen as follows: $\xi_o=\xi_1=\xi_2=\xi_3=1/8$, $\xi_l=0.5/(l+1)$ for $l>3$. When calculating the resonances associated with the $N=5$ positronium threshold, we choose the following values for the nonlinear parameters: $\xi_o=\xi_1=\xi_2=\xi_3=\xi_4=1/10$, $\xi_l=0.5/(l+1)$ for $l>4$.

In the complex-rotation method [24], the radial coordinates are transformed according to the rule

$$r \rightarrow r \exp(i\theta), \tag{5}$$

where θ is the so-called rotation angle. Under this transformation the Hamiltonian given by the Eq. (1) assumes the form

$$H = T \exp(-2i\theta) + V \exp(-i\theta). \tag{6}$$

The eigenvalues are obtained by solving the complex-eigenvalue problem.

$$E = \frac{\langle \Psi H \Psi \rangle}{\langle \Psi \Psi \rangle}. \tag{7}$$

A resonance eigenvalue is an eigenvalue which does not vary when the rotation angle θ changes. In practice, due to finite-basis effects resonance eigenvalues exhibit slow dependence on the rotation angle. Therefore, the resonance eigenvalues are ones for which $|\partial E/\partial\theta|$ assumes minimal value. Following this strategy one obtains the complex energy of a resonance state

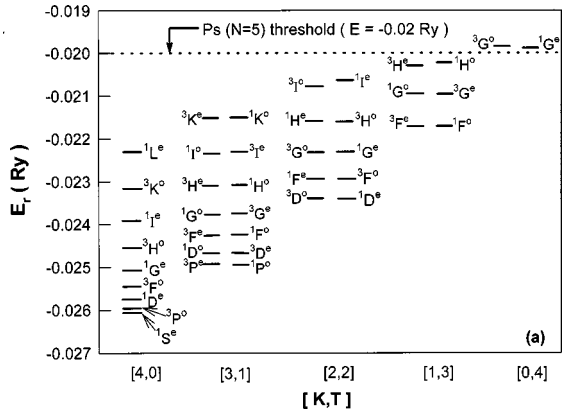

FIG. 4. Rotational character of the spectra of the doubly excited intrashell states of Ps^- associated with the Ps ($N=5$) threshold, rotor series with $K+T=4$ are presented.

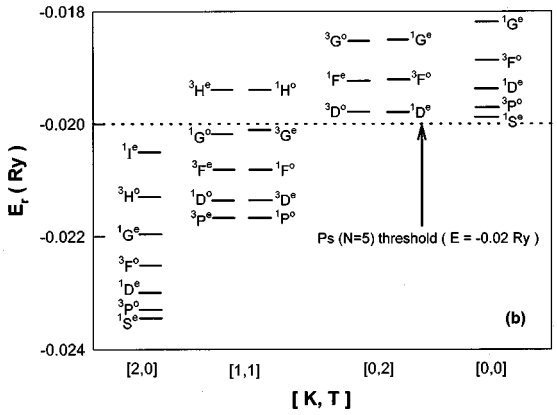

FIG. 5. Rotational character of the spectra of the doubly excited intrashell states of Ps^- associated with the Ps ($N=5$) threshold, rotor series with $K+T=2$ are presented.

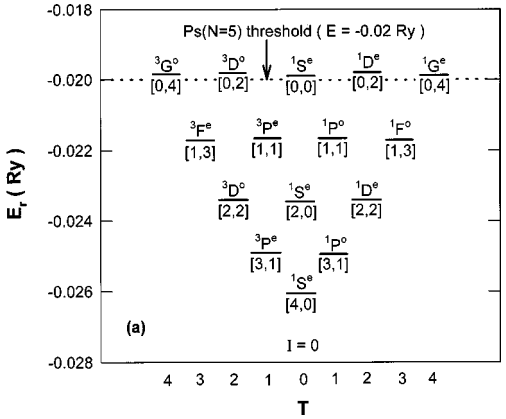

FIG. 6. Vibrational character of the spectra of the doubly excited intrashell states of Ps^- associated with the Ps ($N=5$) threshold. States with $I=0$ are presented.

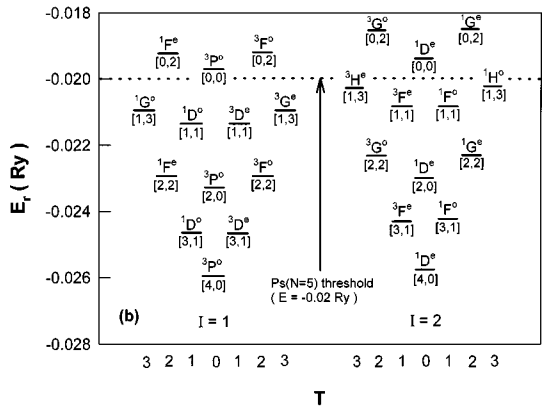

FIG. 7. Vibrational character of the spectra of the doubly excited intrashell states of Ps^- associated with the Ps ($N=5$) threshold. States with $I=1,2$ are presented.

$$E_{\rm res}=E_r-i\Gamma/2, \tag{8}$$

where E_r gives the resonance position and Γ the width of the resonance.

III. NUMERICAL RESULTS

To find the optimum value of the rotation angle θ in the formula (6) the following strategy has been adopted in the work. The Hamiltonian matrix has been repeatedly calculated and diagonalized for several values of θ. The range of the θ values for which the calculations have been performed depended upon the nature of the resonance considered. In the case of a Feshbach resonance the Hamiltonian matrix has been calculated and diagonalized for the following set of θ values: $\theta=0.20,0.25,0.30,0.35,0.40,0.45$. After diagonalization of the energy matrix for this set of θ values, the optimum θ value for a given Feshbach resonance was found as that for which the absolute value of the numerically estimated derivative $\partial E/\partial\theta$ had a minimum as a function of θ. The value of the complex energy calculated for the optimum θ value thus determined was accepted as a complex energy of a resonance, the dispersion of the values of complex energy for the θ values in the vicinity of the optimum θ value provided an estimation of the uncertainty of the calculation.

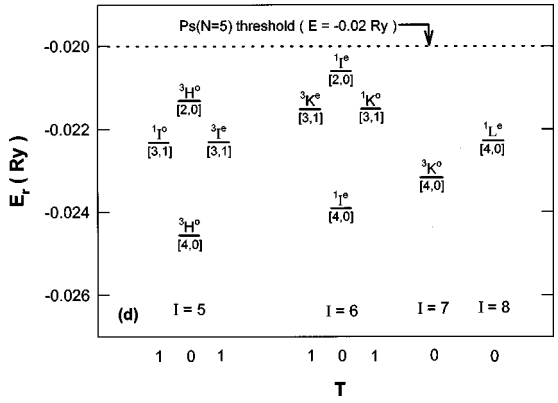

FIG. 9. Vibrational character of the spectra of the doubly excited intrashell states of Ps^- associated with the Ps ($N=5$) threshold. States with $I=5-8$ are presented.

For shape resonances the procedure was entirely analogous save that the range of the θ values for which the Hamiltonian matrix has been calculated was shifted to the larger θ values, so that the energy matrix has been calculated and diagonalized for the following set of θ values: $\theta=0.45,0.50,0.55,0.60,0.65,0.70$. The necessity of such a shift for accurate determination of the parameters of shape resonances has been explained elsewhere [25], and we shall not dwell upon these details here.

Following this strategy we at once obtained resonance positions and widths together with an estimation of the numerical accuracy of our calculation. This estimation applies both to real and imaginary parts of the complex energy. These data are presented in Tables II–IV.

As another confirmation of our estimations of the uncertainties in the resonance parameters calculated in this work, we present in Table I comparison of our data with the results of Hylleraas basis complex-coordinate calculations [12] for the resonances of $^1S^e$ symmetry associated with $N=4$ and $N=5$ positronium thresholds. One can see that the results agree well within the limits of the estimated uncertainty given in the table.

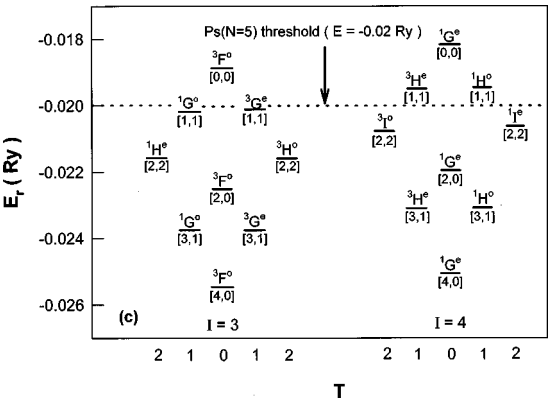

FIG. 8. Vibrational character of the spectra of the doubly excited intrashell states of Ps^- associated with the Ps ($N=5$) threshold. States with $I=3,4$ are presented.

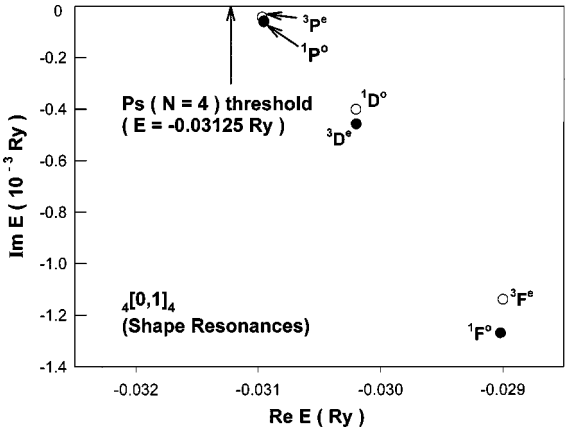

FIG. 10. The resonance poles for the [0,1] shape resonance rotor series associated with the Ps ($N=4$) threshold.

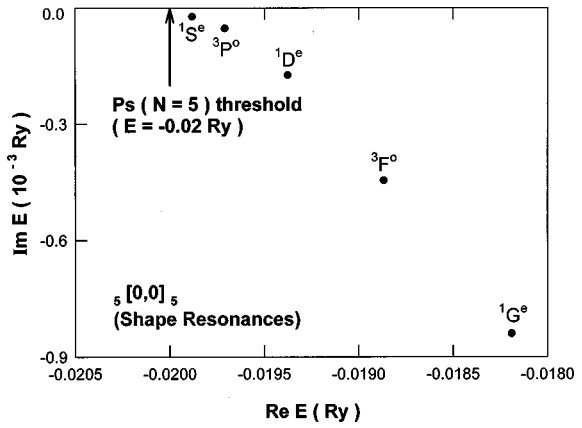

FIG. 11. The resonance poles for the $[0,0]$ shape resonance rotor series associated with the Ps($N=5$) threshold.

IV. DISCUSSION

In Tables II and III the states are classified by the set of quantum numbers (K,T,N,n,L,S,π), where quantum numbers L, S, N, n, and π have the usual spectroscopic meaning. The quantum numbers K and T are ''approximately good'' quantum numbers, and can be described briefly as follows: quantum number K is related to $\langle -\cos\theta_{12}\rangle$, θ_{12} representing the angle between the electron coordinate vectors. The more positive is the value of K, the closer the value of $\langle -\cos\theta_{12}\rangle$ is to unity. In the states having large positive K values the two electrons are located primarily on the opposite sides of the positron. If $K=0$, the coordinate vectors of the two electrons make approximately a right-angle triangle. The quantum number T describes mutual orientation of the orbitals of the two electrons. For example, in the state with $T=0$ the two electrons move on a plane. The quantum numbers K and T hence describe angular correlations between the two doubly excited electrons. For a given set of K, T, and N, the total angular momentum can assume values in the range

$$L=T,T+1,\ldots,K+N-1. \tag{9}$$

The highest L value for a given $[K,T]$ pair is therefore given by the relationship $L_{\max}=K+N-1$. For more detailed discussion of the classification scheme of atomic states based on the quantum numbers K and T readers are referred to Ref. [26]. Figure 1 illustrates the rotational character of the spectrum of the $e^-\ e^+\ e^-$ three-body system. Doubly excited states associated with the Ps($N=4$) threshold are shown. States having the same values of the K and T quantum numbers are grouped together. They belong to the so-called rotor series. Various rotor series are presented in Fig. 1. Instead of the mentioned above set (K,T,N,n,L,S,π) of quantum numbers, we could use more frequently employed set (N,l_1,n,l_2,L,S,π) (where l_1 and l_2 are individual angular momenta of the electrons). For example, the resonances belonging to the $[3,0]$ series shown in the Fig. 1 could be described as $4s^2\ ^1S^e$, $4s4p\ ^3P^o$, $4p^2\ ^1D^e$, $4p4d\ ^3F^o$, $4d^2\ ^1G^e$, $4d4f\ ^3H^o$, and $4f^2\ ^1I^e$. In Figs. 2 and 3 we use the results for the $N=4$ doubly excited intrashell states to construct the I-supermultiplet structures [27]. The quantum number I is defined as

$$I=L-T \tag{10}$$

and has the same meaning as the rovibrational quantum number R used in molecular physics [27]. For example, states with $I=0$ are the ground states of various rotor series. The

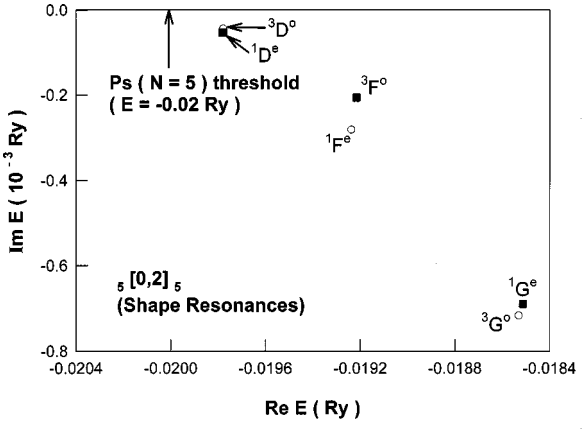

FIG. 12. The resonance poles for the $[0,2]$ shape resonance rotor series associated with the Ps($N=5$) threshold.

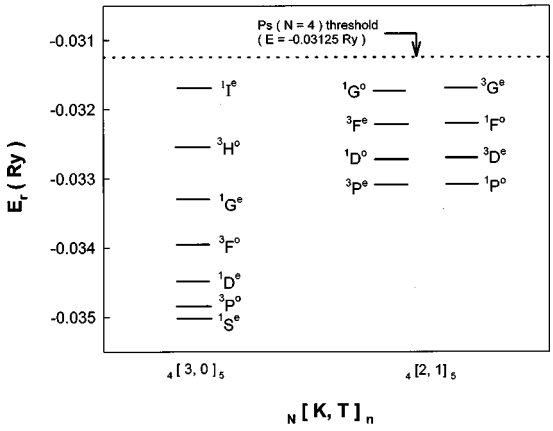

FIG. 13. Rotational character of the spectra of the doubly excited intershell states for the $_4[3,0]_5$ and $_4[2,1]_5$ series.

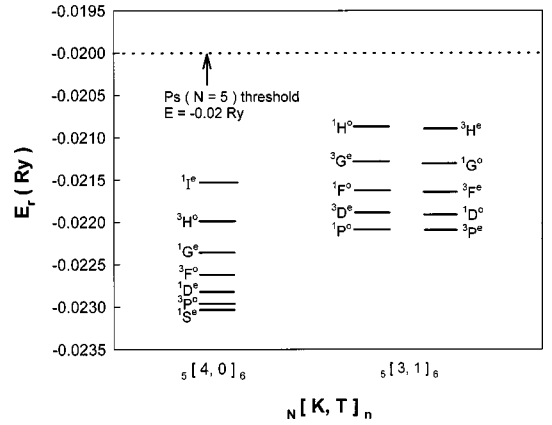

FIG. 14. Rotational character of the spectra of the doubly excited intershell states for the $_5[4,0]_6$ and $_5[3,1]_6$ series.

TABLE IV. Doubly excited intershell states of Ps- associated with the $N=4$ and $N=5$ Ps threshold. The estimated uncertainty in the resonance energy is given in the parentheses.

State	$KTNn$	E_r(Ry)	$\Gamma/2$(Ry)	Resonance
$^1S^e$	3045	-0.0350207 (10^{-7})	1.315×10^{-4}	Feshbach
$^3P^o$	3045	-0.0348422 (10^{-7})	1.172×10^{-4}	Feshbach
$^1D^e$	3045	-0.034496 (10^{-6})	8.5×10^{-5}	Feshbach
$^3F^o$	3045	-0.033967 (5×10^{-6})	5.1×10^{-5}	Feshbach
$^1G^e$	3045	-0.033299 (5×10^{-6})	3.7×10^{-5}	Feshbach
$^3H^o$	3045	-0.03256 (10^{-5})	3.3×10^{-5}	Feshbach
$^1I^e$	3045	-0.03169 (4×10^{-5})	1.8×10^{-4}	Feshbach
$^1P^o$	2145	-0.0330786 (10^{-6})	2.159×10^{-5}	Feshbach
$^3D^e$	2145	-0.0327038 (7×10^{-6})	4.603×10^{-5}	Feshbach
$^1F^o$	2145	-0.0321725 (3×10^{-5})	1.1395×10^{-4}	Feshbach
$^3G^e$	2145	-0.0315998 (4×10^{-5})	1.6020×10^{-4}	Feshbach
$^3P^e$	2145	-0.0330875 (10^{-7})	8.972×10^{-6}	Feshbach
$^1D^o$	2145	-0.0327256 (4×10^{-7})	1.3140×10^{-5}	Feshbach
$^3F^e$	2145	-0.0322207 (10^{-6})	4.6717×10^{-5}	Feshbach
$^1G^o$	2145	-0.0316432 (3×10^{-5})	1.1813×10^{-4}	Feshbach
$^1S^e$	4056	-0.0230390 (10^{-7})	1.164×10^{-4}	Feshbach
$^3P^o$	4056	-0.022967 (10^{-6})	1.14×10^{-4}	Feshbach
$^1D^e$	4056	-0.022822 (8×10^{-6})	9.8×10^{-5}	Feshbach
$^3F^o$	4056	-0.02262 (10^{-5})	1.0×10^{-4}	Feshbach
$^1G^e$	4056	-0.022358 (3×10^{-6})	6.9×10^{-5}	Feshbach
$^3H^o$	4056	-0.02199 (10^{-5})	5.4×10^{-5}	Feshbach
$^1I^e$	4056	-0.02153 (2×10^{-5})	6.5×10^{-5}	Feshbach
$^1P^o$	3156	-0.0220873 (3×10^{-7})	3.04×10^{-5}	Feshbach
$^3D^e$	3156	-0.0218955 (5×10^{-7})	3.62×10^{-5}	Feshbach
$^1F^o$	3156	-0.021622 (5×10^{-6})	5.6×10^{-5}	Feshbach
$^3G^e$	3156	-0.02128 (10^{-5})	8.5×10^{-5}	Feshbach
$^1H^o$	3156	-0.02087 (5×10^{-5})	1.6×10^{-4}	Feshbach
$^3P^e$	3156	-0.02209731 (5×10^{-8})	2.625×10^{-5}	Feshbach
$^1D^o$	3156	-0.0219143 (10^{-7})	2.17×10^{-5}	Feshbach
$^3F^e$	3156	-0.021645 (3×10^{-6})	2.1×10^{-5}	Feshbach
$^1G^o$	3156	-0.02131 (10^{-5})	3.6×10^{-5}	Feshbach
$^3H^e$	3156	-0.02090 (3×10^{-5})	8.6×10^{-5}	Feshbach

vibrational character of Ps^- for the $N=4$ states is clearly demonstrated in Figs. 2 and 3.

From Fig. 1 it can be seen that all the members of the rotor series [0,1] and [0,3] having quantum number $K=0$ are shape resonances [28]. As for the other rotor series with $K\neq0$, the members of these series in general lie below the $N=4$ positronium threshold, and are the Feshbach resonances. An exception is found for the [1,0] series. While the lower members of the series ($^1S^e$,$^3P^o$,$^1D^e$,$^3F^o$) are Feshbach resonances, the highest member of this series, the $^1G^e$ state, is located above the $N=4$ Ps threshold, and is a shape resonance. The results for the doubly excited intrashell states associated with the Ps($N=5$) threshold are presented in Table III. Figures 3 and 5 illustrate the rotational character of the spectra of these states. Figure 4 represents the rotor series with $K+T=4$, and Fig. 5 the rotor series with $K+T=2$. The vibrational character of Ps^- for the states associated with the Ps($N=5$) threshold is illustrated in Figs. 6–9, with Fig. 6 showing the molecular supermultiplet with $I=0$. The $I=1$ and $I=2$ supermultiplets are shown in Fig. 7, 8 and 9 show the molecular supermultiplets of with I values ranging from $I=3$ to $I=4$, and $I=5$ to $I=8$, respectively.

From Figs. 4 and 5 it can be seen that all the members of the rotor series with $K=0$ (i.e., the [0,4], [0,2], and [0,0] series) are shape resonances lying above the Ps($N=5$) threshold. As for the other rotor series with $K\neq0$, most of the resonances belonging to these series are Feshbach resonances lying below the $N=5$ Ps threshold.

Finally, we would like to comment on our results for the shape resonances, and on their physical interpretation. Figure 10 shows the resonance poles for the [0,1] rotor series lying above the Ps ($N=4$) threshold. Figures 11 and 12 show the resonance poles for the [0,0] and [0,2] series, respectively, lying above the Ps($N=5$) threshold. In general, all the shape resonance series exhibit a regular pattern, their widths increasing with their positions as one moves upward along the rotor series. Also, the resonance energy increases with the value of the angular momentum.

This indicates that all the potential curves for various members belonging to the same $[K,T]$ series have quite similar structures. In general, a shape resonance in Ps^- is the result of an electron trapping by the combined effective potential formed by an attractive short-ranged dipole potential due to the degeneracy of the excited Ps states, and a repulsive angular momentum barrier. The autoionization process of such a shape resonance is generally dominated by the tunneling effect. The thickness of the potential barrier decreases as one moves upward along the rotor series. As a result, the electron takes a shorter time to tunnel out, and the width of a shape resonance increases.

The present works also provide results for some doubly excited intershell states (see Fig. 13). In particular, Table IV lists the resonance energies and widths for the ${}_4[3,0]_5$ series below the Ps ($N=4$) threshold. The notation ${}_N[K,T]_n$ is used to describe the series.

Some lower-lying members of the ${}_5[4,0]_6$ and ${}_5[3,1]_6$ are presented in the Table IV, as well as in Fig. 14. It can be observed from Fig. 14 that the rotational character is clearly visible for the doubly excited states even when the two doubly excited electrons occupy different shells.

In summary, we have carried out a complex-coordinate rotation calculation of resonance parameters of the doubly excited states in Ps^- associated with the Ps ($N=4$ and $N=5$) thresholds. Products of Slater orbitals are used to represent the two-electron wave functions. Results are used to construct the supermultiplet structures of doubly excited Ps^-. The triatomic molecular (XYX) character of the spectra of the $e^-\ e^+\ e^-$ system exhibiting rotational and vibrational behavior are illustrated in the work. It is hoped that our findings will stimulate further studies of this interesting three-body atomic system.

ACKNOWLEDGMENT

This work was supported by the National Science Council with Grants No. NSC 88-2112-M-001-023 and No. NSC 89-2112-M-001-013.

[1] Y.K. Ho, Phys. Rev. A **19**, 2347 (1979).
[2] Y.K. Ho, Phys. Lett. **102A**, 348 (1984).
[3] S.J. Ward, J.W. Humberston, and M.R.C. McDowell, J. Phys. B **20**, 127 (1987).
[4] J. Botero, Phys. Rev. A **35**, 36 (1987); Z. Phys. D **8**, 177 (1988).
[5] J.M. Rost and D. Wingten, Phys. Rev. Lett. **69**, 2499 (1992).
[6] Y. Zhou and C.D. Lin, Phys. Rev. Lett. **75**, 2296 (1995).
[7] I. Shimamura (unpublished).
[8] A.P. Mills, Jr., Phys. Rev. A **24**, 3242 (1981).
[9] A.K. Bhatia and R.J. Drachman, Phys. Rev. A **28**, 2523 (1983); **35**, 4051 (1987).
[10] J. Botero and C.H. Greene, Phys. Rev. A **32**, 1249 (1985); Phys. Rev. Lett. **56**, 1366 (1986).
[11] Y.K. Ho and A.K. Bhatia, Phys. Rev. A **45**, 6268 (1992).
[12] Y.K. Ho, Chin. J. Phys. (Taipei) **35**, 97 (1997).
[13] A.K. Bhatia and Y.K. Ho, Phys. Rev. A **42**, 1119 (1990); Y.K. Ho and A.K. Bhatia, *ibid.* **44**, 2890 (1991).
[14] A.K. Bhatia and Y.K. Ho, Phys. Rev. A **48**, 264 (1993).
[15] Y.K. Ho and A.K. Bhatia, Phys. Rev. A **50**, 2155 (1994).
[16] A.P. Mills, Jr., Phys. Rev. Lett. **46**, 717 (1981).
[17] A.P. Mills, Jr., Phys. Rev. Lett. **50**, 671 (1983); A. P. Mills, Jr., in *Annihilation in Gases and Galaxies, NASA Conference Publication No. 3058*, edited by R. J. Drachman (NASA, Washington, DC, 1990), p. 213.
[18] I. Ivanov and Y.K. Ho, Phys. Rev. A **60**, 1015 (1999).
[19] E.A. Wheeler, Ann. (N.Y.) Acad. Sci. **48**, 219 (1946); Y.K. Ho, Phys. Rev. A **48**, 4780 (1993); H. Cox, P.E. Sinclair, S.J. Smith, and B.T. Sutcliffe, Mol. Phys. **87**, 399 (1996); A. Frolov and V. Smith, J. Phys. B **28**, L449 (1995).
[20] D. M. Schrader, in *Positron Annihilation*, edited by P. G. Coleman, S. C. Sharma, and L. M. Diana (North-Holland, Amsterdam, 1982), p. 71.
[21] R. J. Drachman, in *Atomic Physics with Positrons*, edited by J. W. Humberston and E. A. G. Armour (Plenum, New York, 1987), p. 203.
[22] Y. K. Ho, in *Annihilation in Gases and Galaxies* (Ref. [17]).
[23] Y.K. Ho, Hyperfine Interact. **89**, 401 (1994).
[24] Y.K. Ho, Phys. Rep. **99**, 1 (1983); W.P. Reinhardt, Annu. Rev. Phys. Chem. **33**, 223 (1982), and references therein.
[25] Y.K. Ho, Phys. Lett. A **189**, 374 (1994); Y.K. Ho, Phys. Rev. A **49**, 3659 (1994).
[26] D.R. Herrick, Adv. Chem. Phys. **52**, 1 (1983); C.D. Lin, Adv. At. Mol. Phys. **22**, 77 (1983).
[27] M.E. Kellman and D.R. Herrick, Phys. Rev. A **28**, 2523 (1983); **35**, 4051 (1987).
[28] J.M. Rost, Hyperfine Interact. **89**, 343 (1994).